Neuron, Vol. 20, 671–682, June, 2000, Copyright ©2000 by Cell Press

Selective Depression of Low–Release Probability Excitatory Synapses by Sodium Channel Blockers

Murali Prakriya† and Steven Mennerick*
Departments of Psychiatry and
Anatomy and Neurobiology
Washington University School of Medicine
St. Louis, Missouri 63110

Summary

Sodium channels (NaChs) play a central role in action potential generation and are uniquely poised to influence the efficacy of transmitter release. We evaluated the effect of partial NaCh blockade on two aspects of synaptic efficacy. First, we evaluated whether NaCh blockade accounts for the ability of certain drugs to selectively depress glutamate release. Second, we evaluated the contribution of NaChs to intraneuronal variability in glutamate release probability (p_r). The anti-glutamate drug riluzole nearly completely depresses glutamate excitatory postsynaptic currents (EPSCs) at concentrations that barely affect GABAergic inhibitory postsynaptic currents (IPSCs). NaCh inhibition explains the selective depression. Unlike other presynaptic depressants, partial NaCh blockade increases paired-pulse EPSC depression. This result is explained by selective depression of low-p_r synapses. We conclude that local variations in the action potential contribute to p_r variability among excitatory synapses.

Introduction

Synaptic transmission is a multistep process in which sodium action potentials propagate along the axon to synaptic terminals, resulting in Ca^{2+} influx through voltage-gated Ca^{2+} channels and exocytosis of transmitter-filled vesicles. Recently, it has become clear that the effectiveness of synaptic transmission in response to action potentials is variable. Large differences in synaptic output are seen not only between different types of neurons (Msghina et al., 1998) but also between individual synapses of the same neuron (Atwood, 1967; Murthy et al., 1997). There is widespread debate over the potential factors for governing the efficacy and variability of synaptic transmission in the nervous system. Most reports examining the factors underlying variability of transmitter release have focused on the components of the transmitter release machinery at the active zone. These factors include density and open probability of Ca^{2+} channels at the active zone (Msghina et al., 1999), the size of the readily releasable pool of vesicles (Murthy et al., 1997), and the sensitivity of the release machinery to Ca^{2+} (Hsu et al., 1996; Johannes et al., 1998). Surprisingly, despite their ubiquity in neurons and their central role in active signaling, sodium action potentials themselves have received little attention as potential regulators of synaptic efficacy, likely because of the perceived all-or-none nature of action potentials.

One perplexing observation linking sodium channels (NaChs) to synaptic output comes from a class of anticonvulsant, neuroprotective agents that reportedly inhibits glutamate release selectively over release of other neurotransmitters (Leach et al., 1986, 1991; Martin et al., 1993; MacIver et al., 1996). Among the best known and clinically useful compounds are riluzole (2-amino-6-trifluoromethoxybenzothiazole), lamotrigine, and phenytoin. These agents are structurally diverse and have several reported targets, but the drugs share the ability to block voltage-gated sodium currents (Taylor and Meldrum, 1995). It is unclear how inhibition of a ubiquitous target like voltage-gated NaChs might cause selective glutamate release inhibition. Thus, some have questioned the ability of these agents to preferentially depress glutamate release (Taylor and Meldrum, 1995; Umemiya and Berger, 1995; Obrenovitch, 1998).

On the other hand, the ubiquity of NaChs may belie subtle differences in density and/or functional properties of the channels that could produce variability in synaptic output between neurons and among different synapses of the same neuron. Indeed, dendritic NaCh density is substantially higher in hippocampal interneurons than in principal cells (Martina et al., 2000). In addition, there are differences in the density and functional properties of various voltage-gated ion channels, including NaChs, within individual hippocampal neurons (Magee and Johnston, 1995; Colbert and Johnston, 1996; Martina and Jonas, 1997; Stuart et al., 1997). Thus, although sodium action potentials are generally considered all-or-none events, the inactivation status or the local density of voltage-gated channels could influence synaptic effectiveness by altering the action potential waveform in different branches of the axon or by promoting branchpoint failure. Consistent with this idea, recent results have suggested that the synaptic release probability (p_r) covaries more strongly in adjacent synaptic terminals than in physically distant ones (Murthy et al., 1997).

Here, we examine two aspects of NaChs' potential role in governing and modulating synaptic transmitter release. First, we evaluate whether NaCh blockade can account for the putative ability of certain drugs to selectively depress glutamate release over release of the major inhibitory neurotransmitter GABA (Leach et al., 1986, 1991; Martin et al., 1993; MacIver et al., 1996). Second, we evaluate whether local variation in NaCh function might participate in the recently observed variability in vesicular glutamate p_r at different synaptic terminals of an axon (Rosenmund et al., 1993; Murthy et al., 1997). Our results suggest that NaCh inhibition is responsible for the selective depression of glutamate release by anti-glutamate drugs and suggest fundamental differences in the efficacy of excitation/secretion coupling between excitatory and inhibitory neurons. In addition, our results suggest that the excitatory postsynaptic current (EPSC)

*To whom correspondence should be addressed (e-mail: menneris@psychiatry.wustl.edu).
†Present address: Department of Molecular and Cellular Physiology, Stanford University, Stanford, California 94305.

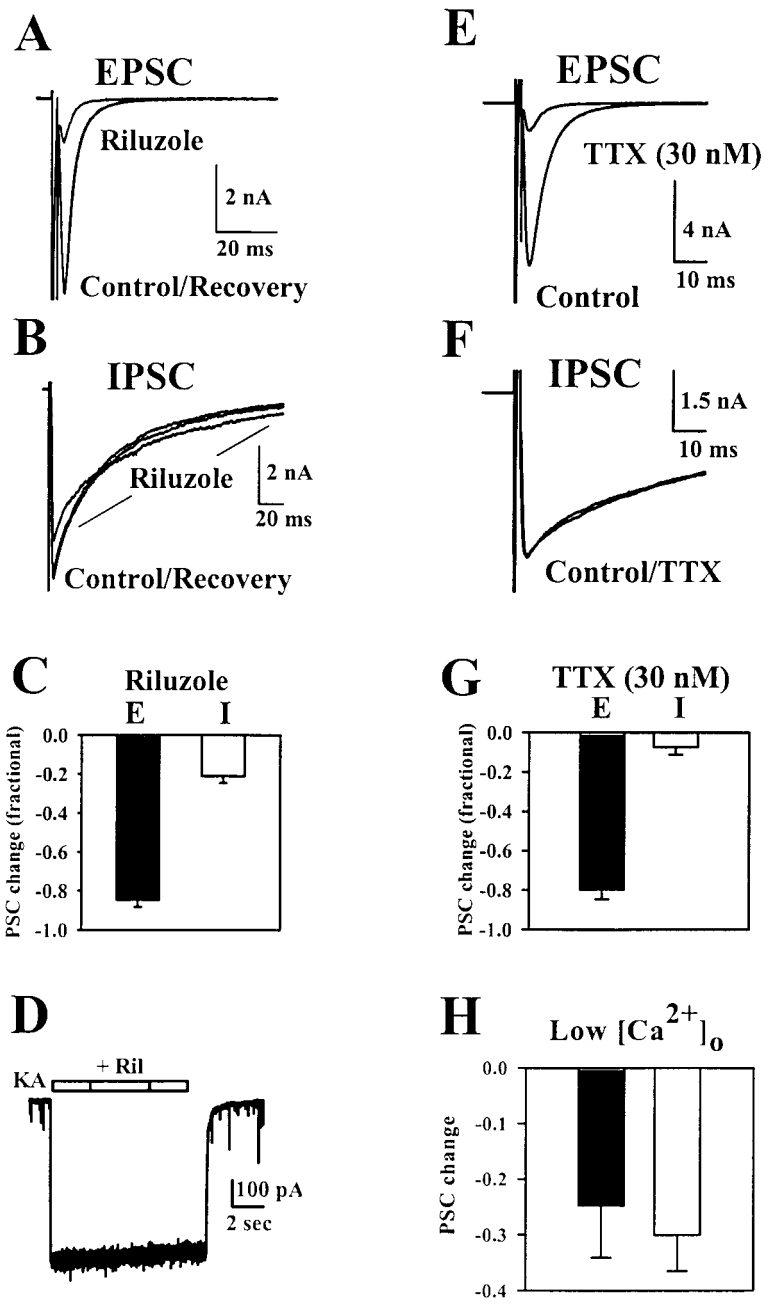

Figure 1. The Putative Selective Glutamate Release Inhibitor Riluzole Preferentially Depresses EPSCs

(A) Autaptic AMPA receptor–mediated EPSC from a solitary excitatory neuron in the presence and absence of riluzole. Fast initial transients represent capacitive and ionic currents in response to stimulation and have been truncated in this and subsequent figures. When 20.0 μM riluzole was included in the bath solution, the EPSC was severely depressed but recovered by the next stimulus, delivered in control saline 20 s later.

(B) Autaptic $GABA_A$ receptor–mediated IPSC from a solitary GABAergic cell. The same experimental protocol used for the cell in (A) produced only very mild depression of the peak IPSC, with a slight slowing of the IPSC decay.

(C) Summary of the effects of 20.0 μM riluzole on peak PSCs in 10 excitatory neurons and 15 inhibitory neurons.

(D) Riluzole has no significant postsynaptic effects on AMPA receptors. Kainate (50.0 μM) was applied to a hippocampal neuron for the duration indicated by the bar. During the period indicated by the closed bar, 20.0 μM riluzole was coapplied to the cell with kainate.

(E–G) TTX shows differential effects quantitatively similar to those of riluzole.

(E) Effect of 30.0 nM TTX on an autaptic EPSC.

(F) TTX had little effect on the peak amplitude of an autaptic IPSC and no effect on the IPSC time course.

(G) Summary of the effects of 30.0 nM TTX on five EPSCs (closed bar) and five IPSCs (open bar).

(H) Summary of the effects of altering Ca^{2+} influx on EPSCs (closed bar) and IPSCs (open bar). Extracellular Ca^{2+} was lowered from 2.0 mM to 1.5 mM. Extracellular Mg^{2+} was raised from 1.0 mM to 1.5 mM.

depression by partial NaCh blockade selectively targets low-p_r synapses. These results imply that local variations in the action potential waveform may participate in dictating p_r at individual synaptic terminals by shaping the degree of local excitation.

Results

Selective Depression of Excitatory Neurotransmission by a Presynaptic Mechanism

Previous studies reporting preferential depression of glutamate release were based on measurements of glutamate and GABA in hippocampal slices (Martin et al., 1993; MacIver et al., 1996). A disadvantage in these experiments is that indirect effects of the drug via polysynaptic modulatory circuits cannot be ruled out as a possible a mode of action of this drug. Hence, we tested the idea that riluzole selectively and directly depresses excitatory neurotransmission. We used solitary postnatal hippocampal cells grown in microcultures for these experiments. Two important advantages of this experimental preparation for the present studies are the formation of autapses (self synapses) in microculture neurons, allowing the transmitter phenotype of neurons to be readily identified, and the lack of polysynaptic influences on solitary microculture neurons. In solitary excitatory cells, the putative anti-glutamate drug riluzole (20.0 μM) dramatically reduced the peak of the AMPA receptor–

mediated autaptic EPSC (85% ± 4%, n = 10; Figure 1A). Similar effects were observed on NMDA receptor–mediated EPSCs examined in Mg^{2+}-free extracellular saline (see below). In contrast, 20.0 μM riluzole inhibited peak autaptic inhibitory postsynaptic currents (IPSCs) in the same cultures by only 24% ± 7% (n = 15 cells).

Riluzole slightly but reliably prolonged IPSCs (Figure 1B). The 10%–90% decay time of IPSCs increased from 121 ± 15 ms to 156 ± 16 ms in 20.0 μM riluzole ($p < 0.001$, n = 14 cells, paired t test). Although the prolongation of IPSCs by riluzole may contribute to the neuroprotective properties of riluzole, we did not further characterize this effect of riluzole in the present work. Rather, we explored the mechanism of EPSC inhibition by riluzole.

To explore whether riluzole blocks postsynaptic glutamate receptors, thus preferentially depressing EPSCs, we examined neuronal responses to exogenous kainate and NMDA to directly activate non-NMDA and NMDA receptors, respectively (Figure 1D). Riluzole had no effect on kainate responses (0.0% ± 0.2% change, n = 7 cells) or NMDA responses (1.5% ± 1% riluzole-induced increase in responses to 20.0 μM NMDA, n = 4 neurons). Therefore, in hippocampal neurons, the preferential inhibition of EPSCs by riluzole cannot be explained by depression of postsynaptic receptor responsiveness.

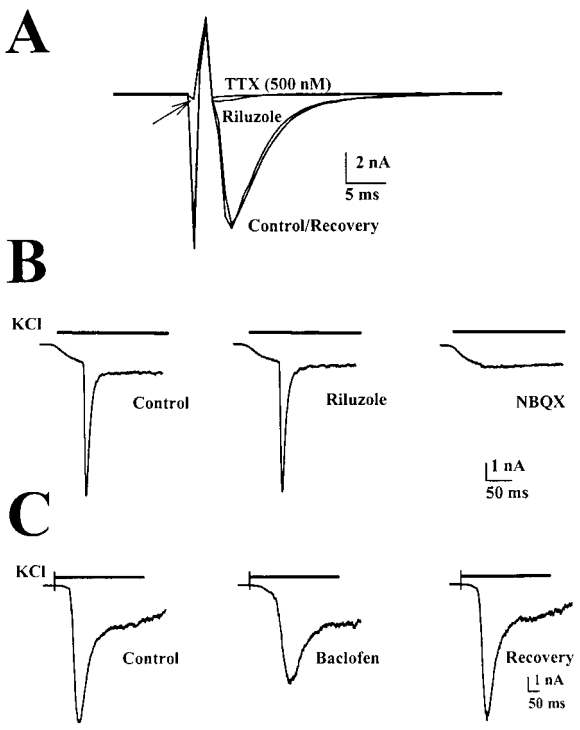

Figure 2. Effect of Riluzole on Glutamate Release in the Absence of Sodium Action Potentials

The data in (A) and (B) are from one excitatory cell. The data in (C) are from another excitatory neuron.

(A) Riluzole (20.0 μM) severely depressed the EPSC, and 500 nM TTX totally abolished the EPSC in response to the standard stimulus protocol. In this expanded trace, the sodium current in response to stimulation is apparent. TTX nearly abolished the sodium current (arrow), while a sizable sodium current was present in the presence of riluzole.

(B) In the presence of 500 nM TTX, autaptic transmission from unclamped synaptic terminals was stimulated with hyperkalemic saline (104 mM potassium, equimolar substitution for sodium) applied for the duration indicated by the thick line above the traces. The middle trace was obtained in the presence of 20.0 μM riluzole. The trace on the far right was obtained in the presence of 5.0 μM NBQX to confirm that the transient current in response to hyperkalemia is due to activation of glutamate receptors.

(C) The $GABA_b$ agonist baclofen (20.0 μM) depressed the hyperkalemia-induced EPSC.

Depression of Sodium Current Explains Selective EPSC Depression

Riluzole has been reported to have multiple effects on ion channels, including inhibition of voltage-gated NaChs (Hebert et al., 1994; Song et al., 1997; Stefani et al., 1997). In hippocampal microcultures, axonal escape from voltage clamp and a resulting action potential are necessary for effective stimulation of evoked transmitter release (Bekkers and Stevens, 1991). Therefore, action potentials and, specifically, NaChs are plausible targets for presynaptic modulators in this preparation. To evaluate whether riluzole's synaptic effects are due to depression of NaCh function, we compared them with the effects of dilute tetrodotoxin (TTX), a highly selective inhibitor of voltage-gated NaChs. Preliminary experiments showed that 30.0 nM TTX yielded EPSC inhibition similar to that of 20.0 μM riluzole, the concentration used in the experiments described in Figures 1A–1C. Surprisingly, we found that this TTX concentration produced preferential depression of excitatory neurotransmission essentially identical to that of riluzole. These results are summarized in Figures 1E–1G. Saturating concentrations of TTX (1.0 μM) abolished both EPSCs and IPSCs (data not shown), consistent with the necessity of sodium action potentials for transmitter release from both cell types.

We also evaluated the effects of three other NaCh blockers at moderate concentrations on glutamate and GABA neurons (n = 7 and 6 neurons, respectively). Lamotrigine (10.0 μM) depressed AMPA receptor–mediated EPSCs by 40% ± 10% and IPSCs by 1% ± 1%. Carbamazepine (50.0 μM) depressed EPSCs by 40% ± 10% and IPSCs by 9% ± 7%. Phenytoin (2.5 μM) depressed EPSCs by 30% ± 8% and IPSCs by 1% ± 1%. The preferential anti-glutamate effect of these drugs suggests that inhibitory and excitatory hippocampal neurons differ fundamentally in the efficacy of excitation/secretion coupling. Although each of these drugs (with the exception of TTX) has reported targets other than voltage-gated NaChs (Taylor and Meldrum, 1995), taken together with the effects of TTX, the results strongly suggest that inhibition of NaChs accounts for the preferential anti-glutamate effect of these drugs.

Riluzole did not affect somatic voltage-gated Ca^{2+} channels, voltage-gated K^+ channels, or resting K^+ conductances (data not shown). In addition, the size of the readily releasable vesicle pool was not affected, as judged from the integrated postsynaptic responses to 600 mM sucrose applications (data not shown). Thus, in hippocampal neurons, voltage-gated NaChs appear to be the primary, if not the only, target responsible for the synaptic effects of riluzole at low micromolar concentrations.

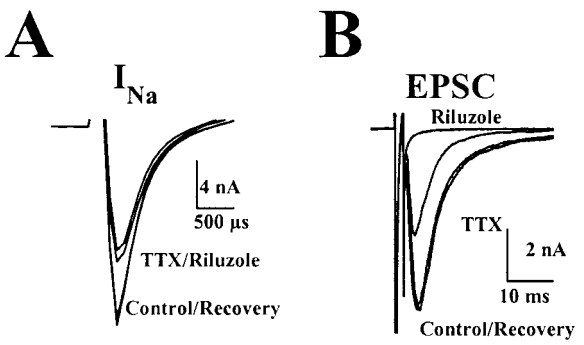

Figure 3. Riluzole Produces a Paradoxically Large EPSC Depression Based on the Amount of Soma Sodium Current Block

(A) Unsubtracted sodium currents recorded during synaptic stimulation of an excitatory neuron. TTX (20.0 nM) produced slightly greater inhibition of the sodium current than did 20.0 μM riluzole.

(B) Same trace as (A), but a longer sweep is displayed to show the EPSC evoked in the various experimental conditions. Note that despite the greater inhibition of sodium current by TTX (A), the EPSC is much more severely depressed by riluzole.

To further determine if events related to calcium influx and exocytosis underlie the difference in susceptibility of glutamate versus GABA-releasing neurons, we evaluated the effect of lowering extracellular [Ca^{2+}] on GABA and glutamate release. There was no difference in the sensitivity of the two cell types to reduced Ca^{2+} influx (Figure 1H). Therefore, differences between cells in the coupling of Ca^{2+} influx to transmitter release do not underlie the preferential effect of partial NaCh block on EPSCs. This experiment is also consistent with the idea that riluzole's preferential effects are through an alteration of the sodium action potential rather than through a direct effect on Ca^{2+} influx.

If riluzole's preferential depression of EPSCs is explained by NaCh blockade, then riluzole should not affect EPSCs evoked by action potential–independent stimuli. In the same neurons in which riluzole severely depressed the electrically evoked EPSC (Figure 2A), we used hyperkalemic solutions (104 mM KCl equimolar substitution for NaCl) in the presence of high concentration of TTX (500 nM) to directly depolarize unclamped axon terminals and evoke glutamate release (Figure 2B). Riluzole did not depress the peak hyperkalemia-induced EPSC in the presence of TTX (114% ± 6% of control, n = 5 cells). In the same experimental protocol, another presynaptic modulator, the $GABA_B$ agonist baclofen, depressed peak hyperkalemia-induced release by 22% ± 4% (n = 8; Figure 2C). These results again exclude an effect of riluzole on postsynaptic AMPA receptors and are consistent with the idea that NaChs are the relevant presynaptic targets of riluzole.

Riluzole's Voltage-Dependent Blockade of NaChs Enhances Its Depression of EPSCs

One initially paradoxical aspect of the conclusion that riluzole acts exclusively through effects on NaChs was apparent when effects of riluzole and TTX on soma sodium current were compared with the effects on EPSCs. We found that 20.0 nM TTX blocked 33% ± 4% of unsubtracted soma sodium current in excitatory neurons, while 20.0 μM riluzole blocked 21% ± 4% (n = 10; Figure 3A). Despite the larger effect of TTX on sodium current, in these same neurons, EPSC amplitude was much more severely depressed by 20.0 μM riluzole than by 20 nM TTX (85% ± 4% versus 43% ± 9%; Figures 3A and 3B).

We reasoned that this result could be reconciled with the conclusion that riluzole's relevant targets are voltage-gated NaChs by hypothesizing that axonal NaChs are more sensitive to riluzole than are soma NaChs. Higher sensitivity of axon NaChs to riluzole could arise from previously described differences in the mechanisms of riluzole and TTX block. TTX is a voltage-independent blocker of sodium current (Taylor and Meldrum, 1995), whereas riluzole is voltage dependent and may act through binding tightly to inactivated NaChs (Hebert et al., 1994). Consistent with these previous results, in nucleated patches excised from the soma of excitatory neurons, 20.0 μM riluzole shifted the steady-state inactivation curve of sodium currents to more hyperpolarized potentials (Figures 4A and 4B). Boltzmann fits to steady-state inactivation data from excitatory neurons suggested a shift in $V_{1/2}$ (half inactivation voltage) of inactivation from −56 mV to −69 mV. Slope factor was 8.9 in control conditions and 10.3 in riluzole. Similar results were observed in nucleated patches excised from inhibitory neurons (Figure 4C). The $V_{1/2}$ shift in inactivation in inhibitory neurons was from −60 mV to −71 mV. The slope factor of the Boltzmann fit was 7.4 in control conditions and 7.3 in riluzole. In addition to demonstrating the voltage dependence of riluzole block, these data suggest a similar sensitivity of GABAergic and glutamatergic NaChs to riluzole, at least at the soma.

Higher sensitivity of the axonal NaChs to riluzole within glutamatergic cells could arise if the resting potential of unclamped axon is depolarized relative to the clamp potential imposed at the cell body (−70 mV). This would increase the number of inactivated NaChs and would render axon channels more sensitive to riluzole than to TTX. While the axon membrane potential cannot be directly controlled, we provided a relative hyperpolarization to distal presynaptic elements with strong hyperpolarizing prepulses applied to the soma before presynaptic stimulation (Figures 4D and 4E). The hyperpolarizing steps did not affect the baseline EPSC amplitude. However, consistent with the idea that the paradoxically strong synaptic riluzole effect may relate to larger fractional block of axonal sodium current, hyperpolarization relieved a large fraction of riluzole-induced EPSC depression (Figure 4D). In contrast, EPSC inhibition by TTX was unaffected by the prepulse (Figure 4E). These results confirm the voltage dependence of riluzole and the voltage independence of TTX block of axon NaChs.

Similar results were obtained by removing extracellular potassium to hyperpolarize unclamped distal presynaptic elements. Decreasing potassium from 4.0 mM to 0.0 mM hyperpolarized the resting potential of neuronal cell bodies from −60 ± 3 mV to −71 ± 5 mV (n = 14 neurons). Removal of potassium had no overall effect on the baseline EPSC amplitude (97% ± 5% change, n = 20 neurons) but diminished the depression induced by 20.0 μM riluzole (79% ± 4% riluzole depression in 4.0 mM K^+, 48% ± 6% riluzole depression in 0.0 mM K^+). There was a small but statistically significant trend toward increased block by TTX block of EPSCs upon

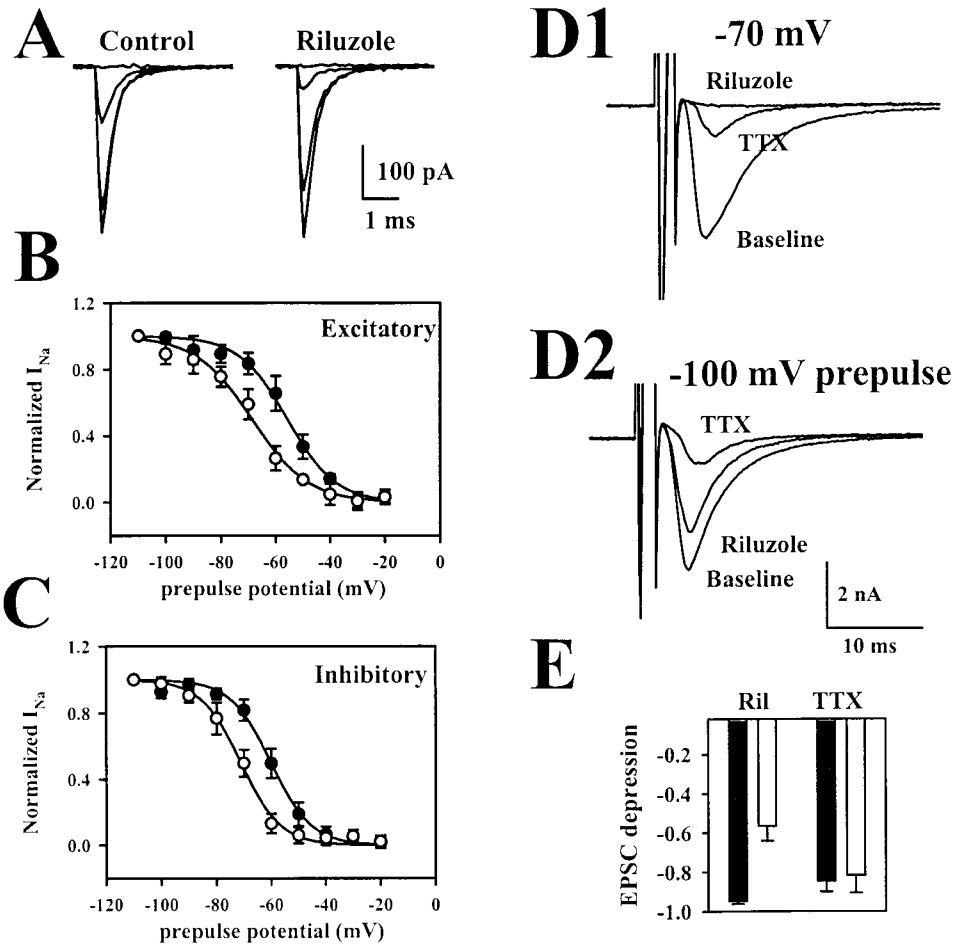

Figure 4. Voltage Dependence of Riluzole Block Can Explain the Paradoxically Large Synaptic Depression

(A) TTX-subtracted sodium currents from a nucleated patch excised from an excitatory neuron.

(Left) Traces represent currents obtained by pulsing the membrane potential to +10 mV from prepulse potentials of −110, −80, −50, and −20 mV in control saline (largest to smallest currents).

(Right) Same series in the presence of 20.0 μM riluzole. Note the lack of effect on sodium currents elicited from the most negative prepulse potentials.

(B) Steady-state inactivation curves obtained from nucleated patches excised from five excitatory neurons. Current size in each patch was normalized to the current elicited from the −110 mV prepulse. Solid lines represent a Boltzmann fit to the steady-state inactivation data (see Results for fit parameters). The form of the Boltzmann equation was $y = 1/(1 + \exp[(V_{1/2} - V)/k])$, where y is the relative response magnitude, $V_{1/2}$ is the half inactivation voltage, V is the prepulse potential, and k is the slope factor.

(C) The same protocols described in (A) and (B) were used to examine the sensitivity of NaChs in inhibitory neurons to riluzole block (n = 5 patches; see Results for fit parameters).

(D and E) Reduction of riluzole block by hyperpolarizing prepulses.

(D1) Riluzole (20.0 μM) caused nearly complete depression of an EPSC using the standard stimulation protocol. TTX (30.0 nM) caused slightly less block of the EPSC.

(D2) In the same neuron, a hyperpolarizing prepulse to −100 mV was applied for 100 ms before the depolarizing stimulus was applied. Following the depolarization, the membrane potential was returned to the standard holding potential of −70 mV so that the driving force on postsynaptic ion channels was not altered from that of the standard protocol. Note that the riluzole effect on the EPSC was reduced, whereas the TTX effect was not. The size of the baseline EPSC was not appreciably altered by the hyperpolarizing prepulse.

(E) Summary data from excitatory cells stimulated with the protocol in D1 (closed bars) and D2 (open bars). Effects of both riluzole (left bars, n = 12) and TTX (right bars, n = 6) are depicted.

potassium removal (41% ± 8% depression in 4.0 mM K^+, 55% ± 8% depression in 0.0 mM K^+, p = 0.02, n = 15). Although the cause of the increased TTX block is unclear, the results, like those of Figures 4D and 4E, suggest that TTX block is not reduced upon hyperpolarization. Taken together, these results are consistent with the idea that axonal channels are more sensitive to riluzole block than are somatic NaChs, possibly because the axon resting potential is more depolarized than is the command potential at the soma.

Evidence that NaCh Density May Partly Determine p_r during Action Potentials at Low-p_r Synapses

We next sought to elucidate the mechanism by which partial NaCh inhibition depresses glutamate release. A common method of probing the mechanism of putative

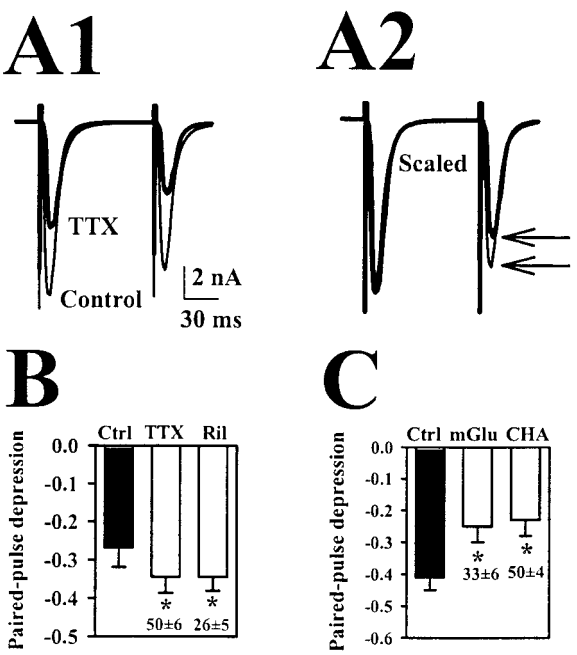

Figure 5. Paired-Pulse Depression Is Increased by NaCh Blockade

(A1) TTX (20.0 nM) block of EPSCs in a paired-stimulation paradigm (100 ms paired-pulse interval). Control traces are thin traces; responses in the presence of TTX are thick traces.

(A2) Same traces, normalized to the control conditioning EPSC to emphasize the increase in paired-pulse depression (arrows).

(B) Summary of the effects of TTX (10–20.0 nM, n = 8 neurons) and riluzole (2.0 μM) on paired-pulse depression. The asterisks indicate $p < 0.05$, paired t test. The means and standard errors associated with the bars represent the degree of conditioning EPSC depression observed in the various conditions.

(C) Summary of the effect of a cocktail of metabotropic glutamate receptor agonists (50.0 μM L-AP4 and 50.0 μM 1S, 3R ACPD [mGlu]) and an adensoine receptor agonist (1.0 μM 2-chloroadenosine [CHA]) on paired-pulse depression of EPSCs.

presynaptic modulators is to examine responses to paired presynaptic stimuli. Paired-pulse stimulation often results in the depression of transmitter release (Magleby, 1987; Zucker, 1989). Depression results primarily from depletion of the readily releasable vesicle pool of vesicles and is especially prominent when the basal p_r is high (e.g., Mennerick and Zorumski, 1995). Presynaptic modulators that decrease p_r also decrease depletion of the releasable pool during conditioning stimulation and therefore decrease paired-pulse depression. Examples of this phenomenon can be seen in the effects of adenosine and metabotropic glutamate receptor agonists on glutamatergic synapses (Hashimoto and Kano, 1998; Kilbride et al., 1998).

Surprisingly, we found that application of 20.0 nM TTX resulted in increased paired-pulse depression at a paired-pulse interval of 100 ms (Figures 5A and 5B). Riluzole at concentrations of 2–10.0 μM also elicited very similar effects (Figure 5B). Note that increased paired-pulse depression elicited by riluzole cannot be explained by riluzole's use dependence (Hebert et al., 1994) because the voltage-independent blocker TTX caused a similar increase in paired-pulse depression (Figures 5A and 5B).

In contrast to the effects of TTX and riluzole, application of 2-chloroadenosine (1.0 μM) or a cocktail of the metabotropic glutamate receptor agonists 1S, 3R ACPD, and L-AP4 (50.0 μM each) decreased paired-pulse depression at hippocampal synapses, as expected of presynaptic depressants (Mennerick and Zorumski, 1995; Hashimoto and Kano, 1998; Kilbride et al., 1998). Depression of the conditioning EPSC with these treatments was similar to that produced by the concentrations of TTX or riluzole employed (Figure 5C). Thus, the effect of partial NaCh blockade is the opposite of that predicted by the actions of adensosine and metabotropic glutamate receptor agonists.

What is a possible mechanism for the increased paired-pulse depression during partial NaCh block? As discussed above, an increased paired-pulse depression suggests an increase in the mean initial p_r. Individual synapses of hippocampal neurons display a wide variability in p_r (Rosenmund et al., 1993; Murthy et al., 1997). We hypothesized that increased paired-pulse depression could result if partial NaCh blockade selectively eliminated the contributions of low-p_r synapses, leaving contributions of high-p_r synapses relatively intact. To directly examine this idea, we took advantage of the ability of the irreversible NMDA receptor blocker MK-801 to selectively inhibit activated NMDA receptors (Huettner and Bean, 1988). Using MK-801, previous experiments have distinguished at least two populations of hippocampal synaptic terminals differing 6-fold in p_r (Hessler et al., 1993; Rosenmund et al., 1993). High-p_r synapses are preferentially susceptible to early block during repeated stimulation in the presence of MK-801, while low-p_r synapses are blocked primarily with later stimuli (Hessler et al., 1993; Rosenmund et al., 1993). Brief applications of MK-801 should reduce the contribution of high-p_r synapses to EPSCs. Therefore, if partial NaCh blockade selectively depresses low-p_r synapses, then the EPSC depression due to partial NaCh blockade should increase after MK-801 treatment.

We therefore examined EPSC block by riluzole before and after MK-801 treatment. Preferential block of NMDA receptors at high-p_r synapses was induced by applying three to eight synaptic stimuli in the presence of 10.0 μM MK-801, an amount sufficient to reduce the EPSC amplitude by 67% ± 4% (n = 7). Riluzole block of NMDA EPSCs increased significantly after MK-801 treatment (37% ± 3% before MK-801 to 60% ± 4% after MK-801; Figures 6A and 6B). In contrast, there was no significant difference in the amount of riluzole block of AMPA responses in these same cells before and after MK-801 treatment (Figures 6A and 6B), thus excluding nonspecific time or stimulus-dependent changes in riluzole sensitivity. Very similar results were obtained with the voltage-independent blocker TTX (Figure 6C). TTX block increased from 22% ± 5% to 31% ± 4% after MK-801. This result indicates that partial blockade of NaChs preferentially inhibits synaptic release from low-p_r synapses.

These results suggest that partial NaCh block may produce unequal effects on the sodium action potential in different synapses and therefore preferentially inhibit release from some synapses. However, it is also possible that partial NaCh block affects all synapses equally,

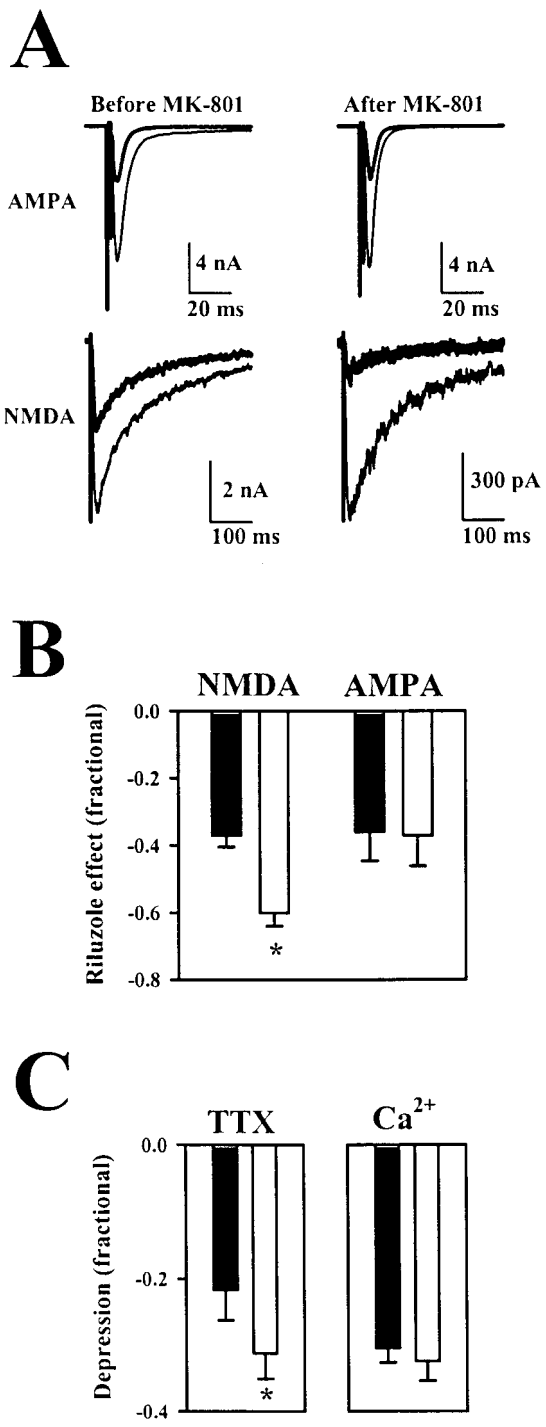

Figure 6. Evidence that NaCh Blockade Preferentially Targets Low-p_r Synapses

(A) The top traces represent AMPA receptor–mediated EPSCs; the bottom traces represent NMDA receptor–mediated EPSCs from the same cell. For both sets of traces, the extracellular saline contained 3.0 mM Ca^{2+}, no added Mg^{2+}, and 10.0 μM glycine. In separate experiments, removing Mg^{2+} had a relatively minor effect on isolated AMPA EPSCs (16% ± 6% increase in EPSC, n = 3). AMPA receptor–mediated EPSCs were isolated using 50.0 μM D-APV. NMDA EPSCs were isolated by omitting D-APV and including 1.0 μM NBQX. Thin traces represent control EPSCs; thick traces represent EPSCs in the presence of 2.5 μM riluzole. Between the left traces and right traces, five stimuli in the presence of 10.0 μM MK-801 were delivered. Note the change in scale of the NMDA EPSCs and the increase in riluzole effect after MK-801 treatment.

(B) Summary of the effect of riluzole before MK-801 treatment (closed bars) and after MK-801 treatment (open bars) on NMDA and AMPA receptor–mediated EPSCs (n = 7 neurons).

(C) Summary of the effect before (closed bars) and after (open bars) MK-801 treatment of TTX (15.0 nM, $p < 0.005$, n = 8, paired t test) and decreased extracellular Ca^{2+} (1.8 mM from 3.0 mM, $p > 0.5$, n = 7) on NMDA receptor–mediated EPSCs.

but reduced Ca^{2+} entry during NaCh block might preferentially target low-p_r synapses because low-p_r synapse have inherently reduced Ca^{2+} entry or poor coupling of Ca^{2+} entry with exocytosis. If susceptible synapses have inherently low p_r, then synaptic depression produced by altering Ca^{2+} influx should also selectively target low-p_r synapses. In contrast to this prediction, we found that synaptic depression caused by reducing $[Ca^{2+}]_o$ from 3.0 mM to 1.8 mM, although similar in magnitude to that produced by dilute TTX or riluzole, did not significantly increase after MK-801 treatment (Figure 6C). Thus, differences in sodium action potentials at different synapses are likely responsible for the differential effects of partial NaCh block on release from different sites on the same presynaptic cell.

Is the Effect on EPSCs by Partial NaCh Block Due to Branch Failure or to Alteration of the Action Potential Waveform?

Partial NaCh block might depress EPSCs by either of two mechanisms. Partial NaCh block could produce branchpoint failure by eliminating action potential invasion of axon branches or synaptic terminals. Alternatively, the action potential waveform may be altered in some axonal branches or synapses, such that Ca^{2+} influx is substantially reduced at the affected synapses. While these two possibilities are not necessarily mutually exclusive, we addressed the likely contribution of each mechanism with the experiments depicted in Figure 7.

If branch failure is responsible for the effect of dilute NaCh blockers on EPSCs, then decreasing (hyperpolarizing) action potential threshold should partially reverse the effect of TTX. TTX (10.0 nM) increased somatic action potential threshold by 6.1 ± 0.9 mV in seven neurons (data not shown). If the synaptic effects of TTX are primarily mediated by branchpoint failure, reversing this effect on threshold should partially compensate for the effect of TTX on EPSCs. To manipulate action potential threshold, we altered the concentration of divalent cations in the extracellular saline to alter surface potential (Hille, 1992). Decreasing the divalent cation concentrations from 2.0 mM Ca^{2+} and 2.0 mM Mg^{2+} (2–2 saline) to 1.1 mM Ca^{2+} and 0.0 mM Mg^{2+} (1.1–0 saline) hyperpolarized action potential threshold by 5.8 ± 0.3 mV without altering action potential peak (0.2 ± 0.2 mV change, $p > 0.05$) or width (0.0 ± 0.1 ms change, $p > 0.05$ change, n = 5 neurons).

By decreasing both Ca^{2+} and Mg^{2+}, we achieved conditions that maintained a similar inherent p_r (in the absence of action potentials), assessed by KCl-evoked EPSCs in the presence of 500 nM TTX (Figure 7B). Consistent with the similar efficacy of KCl-evoked transmitter release, action potential–evoked EPSCs were similar

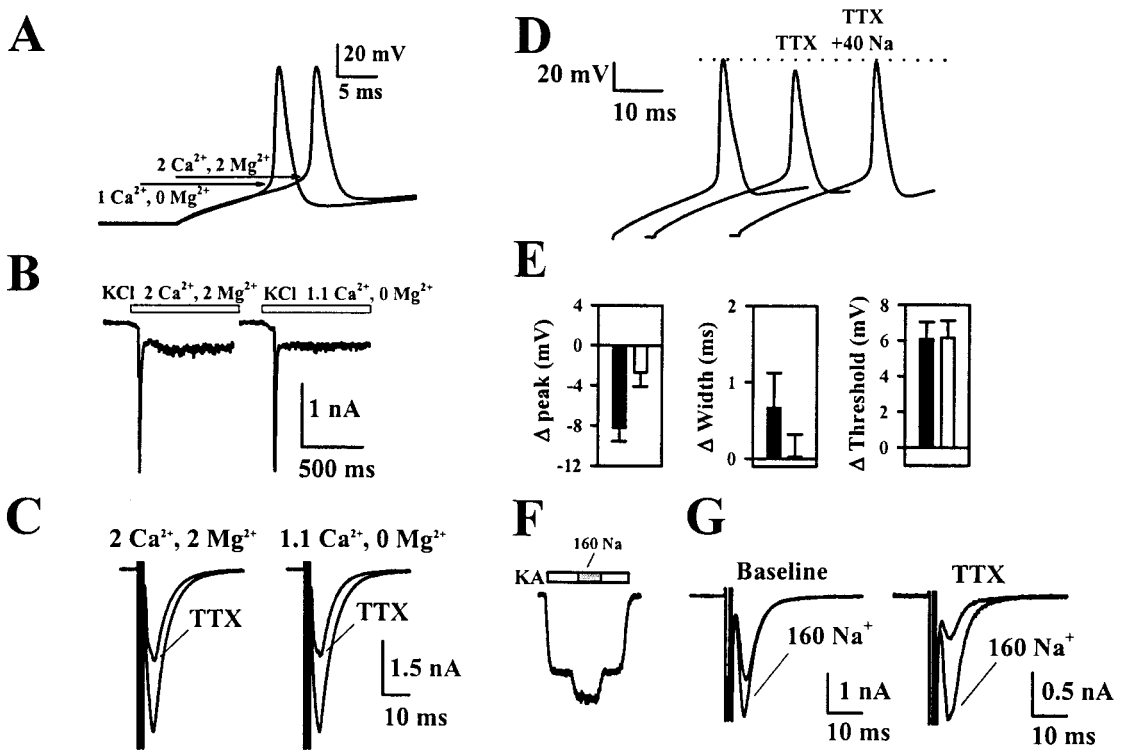

Figure 7. Alteration of Action Potential Waveform but Not Action Potential Threshold Partially Reverses the Effect of Dilute TTX

(A) Decreasing the extracellular divalent cation concentration decreased action potential threshold but did not alter the action potential shape. Threshold is indicated by the arrows. The numbers associated with the divalent cations represent concentrations in millimolars. See Results for a summary of effects on action potential waveform.

(B) The same decrease in divalent cation concentration does not substantially alter transmitter release elicited by KCl. TTX (500 nM) was present throughout. The experimental protocol was the same as that used for Figure 2. The open bar denotes the timing of the KCl application.

(C) The decrease in divalents did not alter action potential–mediated release and did not reduce the degree of TTX (10.0 nM) block of EPSCs.

(D–F) Effect of overcoming TTX effects on action potential waveform.

(D) In the presence of 120 mM Na^+ and 40.0 mM choline, TTX (10.0 nM) slightly inhibited the peak of the action potential. The alteration was overcome by increasing $[Na^+]_o$ to 160 mM (and omitting choline). The dotted line indicates action potential peak in 120 mM Na^+.

(E) Summary of the effect of increasing Na^+ on the alterations in action potential waveform induced by 10.0 nM TTX. Differences (Δ) in the graphs were obtained by subtracting the peak, width, and threshold values of action potentials in 120 mM Na^+ from action potentials in the presence of 120 mM Na^+ plus TTX (10.0 nM, closed bars) and 160 mM Na^+ plus TTX (10.0 nM, open bars).

(F) Effect of increased $[Na^+]_o$ on postsynaptic currents. Na^+ solution (160 nM) increased the response to 20.0 μM kainate (KA) by ~36% compared with responses in 120 mM Na^+. Kainate application is denoted by the horizontal bar. The period during which Na^+ was raised is indicated by the shaded bar.

(G) (Left) EPSCs were similarly affected by increased Na^+.

(Right) In the presence of 10.0 nM TTX, the effect of raising extracellular Na^+ on EPSC amplitude was much larger, suggesting that increased Na^+ partially overcomes the effect of TTX on EPSCs.

in the 2–2 saline and 1.1–0 saline (within 7% ± 3%, n = 13 cells). Importantly, despite the decrease of action potential threshold in 1.1–0 saline, TTX-induced EPSC depression was not decreased in 1.1–0 saline (Figure 7C). In fact, the average effect of TTX was slightly increased in 1.1–0 saline from 22% ± 5% to 31% ± 7% ($p < 0.05$). This result is inconsistent with action potential failure playing an important role in EPSC depression by dilute TTX, although it does not entirely exclude it.

In contrast to action potential failure, if more subtle alterations of the action potential waveform are important in the synaptic effect of NaCh blockers, then a manipulation that reverses the effect of TTX on the action potential waveform should provide partial rescue from effects of TTX on EPSCs. By raising the driving force on extracellular Na^+ and therefore enhancing the current through unblocked NaChs, an elevated $[Na^+]_o$ should overcome the effects of dilute TTX. Raising $[Na^+]_o$ from 120 mM (plus 40.0 mM choline chloride to maintain osmolarity and charge) to 160 mM partially reversed the effects of 10.0 nM TTX on soma action potential height and width (Figures 7D and 7E) but did not alter the effect of TTX on action potential threshold (Figures 7D and 7E). Raising $[Na^+]_o$ by itself increased peak action potential height by 6.3 ± 0.3 mV but also decreased the action potential width by 0.41 ± 0.03 ms ($p < 0.05$, n = 7 excitatory neurons).

Raising Na^+ by 40.0 mM increased peak control EPSCs by 39% ± 8% (n = 6). However, this increase was indistinguishable from the increase in exogenous kainate-induced currents produced by raising Na^+ (36% ± 4%, n = 7 neurons; Figures 7F and 7G). Therefore, the increase in EPSC amplitude with the increase in Na^+ is accounted for by the increased driving force on Na^+

through postsynaptic receptor channels. In contrast, in the presence of 10.0 nM TTX, the increase in EPSC with increased Na^+ was much more dramatic (200% ± 72%, n = 6 neurons; Figure 7G). Thus, partially reversing the effect of TTX on action potential waveform partially overcame the effect of TTX on synaptic glutamate release. Taken together, the results of Figure 7 strongly suggest an important role for alteration of action potential waveform, but not for branch failure, in the synaptic effects of partial NaCh block. This conclusion is also consistent with recent studies suggesting a high safety factor for branch invasion of CNS axons (Mackenzie and Murphy, 1998).

As a further test of the idea that action potential waveform alteration is important in the effect of partial NaCh block on glutamate release, we attempted to overcome the synaptic effect of 10.0 nM TTX with elevated extracellular Ca^{2+}. We reasoned that increasing the driving force on Ca^{2+} should overcome the effect of TTX, but only if an action potential continues to invade susceptible synaptic terminals in the presence of TTX. The branchpoint failure hypothesis, in contrast, would predict that increasing extracellular Ca^{2+} should have no effect on TTX-induced EPSC depression. Consistent with the experiments shown in Figure 7, we found that increasing Ca^{2+} from 2.0 mM to 3.0 mM (Mg^{2+} constant at 1.0 mM) potentiated EPSCs by 18% ± 2% in the absence of TTX but potentiated EPSCs by 45% ± 6% in the presence of TTX (n = 12; data not shown). In these experiments, TTX alone in 2.0 mM Ca^{2+} depressed EPSCs by 59% ± 6%. In summary, these results support the idea that partial NaCh block results in alteration of the action potential waveform at the synapse rather than in failure of action potential invasion. These experiments are also consistent with the idea that TTX most effectively blocks low-p_r synapses (Figures 5 and 6). Under conditions of high p_r (raised extracellular calcium in these experiments), TTX was less effective in blocking glutamate release.

Discussion

We provide evidence that at subsaturating concentrations, NaCh antagonists selectively depress glutamate over GABA release in hippocampal neurons. The selective depression of excitatory neurotransmission by NaCh inhibition implies that excitatory and inhibitory cells differ fundamentally in the efficacy of excitation/secretion coupling. Investigation of the mechanism by which partial NaCh inhibition results in EPSC depression strongly suggests that NaCh density or other factors influencing the sodium action potential waveform influence p_r at excitatory synapses. These conclusions have implications for both the basic physiology of CNS synapses and the mechanisms of clinically important drugs.

Selective Inhibition of Excitatory Neurotransmission by Partial NaCh Blockade

NaCh inhibition evokes dramatically different effects on neurotransmission by excitatory and inhibitory hippocampal neurons. Riluzole was chosen as a prototype voltage-dependent NaCh blocker (Taylor and Meldrum, 1995) because of its reported anti-glutamate effects (Martin et al., 1993; MacIver et al., 1996) and its reported efficacy in treating amyotrophic lateral sclerosis, a disorder possibly involving glutamate-mediated degeneration of motor neurons (Louvel et al., 1997). Previous studies examining differential effects of riluzole on transmitter release in excitatory versus inhibitory neurons were performed in slices (Martin et al., 1993; MacIver et al., 1996). The issue of whether glutamate release is directly affected by riluzole was ambiguous in these studies because of the possibility that other neuromodulatory transmitter systems impinging on the glutamatergic cells might be the relevant targets of riluzole. Combined with previous results, our results with solitary neurons clearly demonstrate that preferential depression of glutamate release is explained by a direct effect of riluzole on glutamatergic cells.

Riluzole may have cellular targets other than NaChs (Debono et al., 1993; Hebert et al., 1994; Huang et al., 1997; Fink et al., 1998). However, in our experiments, soma calcium currents, soma potassium currents, and postsynaptic glutamate receptors were unaffected by riluzole. Dilute concentrations of many different types of NaCh inhibitors all exhibit similar preferential depression of EPSCs, and we detected no effect of riluzole on glutamate released in the absence of sodium action potentials. Finally, the selective NaCh blocker TTX exhibited all of the same essential effects on synaptic responses as riluzole. Thus, NaCh inhibition is clearly sufficient to explain the differential effect of riluzole at low micromolar concentrations, and targets other than NaChs need not be invoked to explain the anti-glutamate properties of riluzole. Because NaCh blockers are important clinical anticonvulsants (Taylor and Meldrum, 1995), the selective anti-glutamate action of these drugs may be an important, underappreciated anticonvulsant mechanism.

There are several possible mechanisms that may underlie the differential effects of NaCh blockers on glutamate versus GABA release. Because the voltage-independent NaCh blocker TTX has a differential effect on EPSCs similar to that of voltage-dependent blockers, it is unlikely that differences in the resting potential and steady-state inactivation status of excitatory versus inhibitory axons explain the differential depression of EPSCs. Also, NaChs from inhibitory neurons, at least at the cell body, are not less sensitive to pharmacological blockade than are channels from excitatory neurons (Figure 4C). Rather, GABAergic hippocampal neurons exhibit a fundamental difference from glutamatergic cells in the efficacy of depolarization/secretion coupling. This may arise from differences in the passive membrane properties or axonal branching patterns of interneurons, differences in the functional density of NaChs in interneuron axons, or differences in the functional coupling of sodium action potentials to calcium influx and transmitter release.

While the precise contribution of these factors awaits further study, a recent report suggested that NaCh density in the dendrites of hippocampal inhibitory interneurons is substantially higher than is the density in dendrites of cortical principal excitatory neurons (Martina et al., 2000). Further, somatodendritic action potential propagation in the interneurons was fast and highly reliable,

and exhibited little attenuation. In contrast, action potential propagation in cortical principal cells is slow and unreliable, and attenuates (Stuart and Sakmann, 1994). This finding raises the strong possibility that the higher safety factor for NaCh blockade in inhibitory neurons observed in our study might arise from differences in the density of axonal NaChs between inhibitory and excitatory neurons.

Preferential Inhibition of Low-p_r Excitatory Synapses by Partial NaCh Blockade

Although synaptic release probability is of fundamental importance to understanding neuronal communication, the factors influencing p_r are not well understood. Sodium action potentials may appear to be unlikely participants in setting release efficacy because of the perception that action potentials are all-or-none phenomena. However, regional differences in sodium action potentials or in susceptibility to action potential invasion could influence synaptic effectiveness at different synaptic sites of the same axon. A particularly provocative finding in the current work is that partial NaCh blockade preferentially depresses transmitter release from low-p_r synapses, evidenced by increased paired-pulse depression in the presence of riluzole and TTX, and increased depression of NMDA EPSCs after MK-801-induced suppression of high-p_r synapses. Furthermore, in elevated extracellular Ca^{2+}, which should increase average p_r, partial NaCh blockade was significantly less effective in depressing release. The clear corollary of the finding that partial NaCh block targets low-p_r synapses is that the sodium action potential, and perhaps the NaChs themselves, influence p_r at excitatory synapses and have a larger role in influencing the efficacy of transmitter release than previously realized. Interestingly, the functional density of available NaChs does not appear to be dictated strongly by steady-state inactivation of channels because strong hyperpolarizing prepulses and hypokalemic solutions, both of which diminish riluzole-induced synaptic depression, do not increase the size of baseline EPSCs.

It is possible that a factor other than NaCh density per se plays a critical role in shaping the sodium action potential waveform in different parts of the axon. For instance, potassium channel density, different electrotonic properties of different axonal segments, and the size of synaptic boutons are potential factors for altering the action potential waveform, thus decreasing p_r and rendering associated synapses susceptible to partial NaCh blockade. Bouton size has been correlated with p_r at hippocampal synapses, and small boutons have disproportionately small active zones (Schikorski and Stevens, 1997). If NaChs in boutons are localized preferentially to active zones, the small number of channels in small synapses may be unable to drive the membrane capacitance as effectively as at larger synapses.

Note that our results do not exclude a role for the action potential waveform in setting p_r at inhibitory synapses, but the data suggest that block of a significantly higher fraction of NaChs is necessary to depress GABA release compared with glutamate release. Our results may (but do not necessarily) predict that GABAergic neurons have a higher p_r in response to action potentials than do excitatory neurons. However, other factors besides the sodium action potential surely participate in setting p_r, and these factors could play a relatively stronger role in influencing p_r at GABA synapses.

Our results indicate that partial NaCh block may produce an altered action potential waveform and thereby elicit less Ca^{2+} influx. The effect of partial NaCh blockade could not be rescued by reducing action potential threshold, suggesting that action potential failure is unlikely to be a strong factor in the synaptic effects of dilute TTX. In contrast, increasing Ca^{2+} influx and increasing the sodium driving force to reverse the effects of TTX on action potential waveform both significantly reversed the synaptic depression induced by dilute TTX. Thus, a primary mechanism of partial NaCh block is alteration of the action potential waveform.

In summary, we have shown that partial NaCh blockade has dramatically different effects on the efficacy of transmitter release from two major classes of hippocampal neurons and has differenct effects even at different synapses of the same excitatory axon. A primary mechanism by which glutamate release is depressed by partial NaCh block is through alteration of the action potential waveform. These results demonstrate a strong role for sodium action potentials in influencing p_r and suggest an unappreciated role for NaChs in dictating the efficacy of synaptic transmission.

Experimental Procedures

Hippocampal Cultures

Hippocampi were taken from albino Sprague-Dawley rat pups at postnatal day 1–3 and dissociated by papain and mechanical dispersion as described (Mennerick et al., 1995). Microculture plates were prepared by coating 35.0 mM plastic cultures dishes (Falcon) with a solution of 0.15% agarose. The agarose dried to form a nonpermissive background for cell adhesion. On the agarose layer, small droplets of collagen (0.5 mg/ml) were sprayed with a microatomizer (Thomas Scientific). Cells were seeded on the bottom of a collagen-coated culture dish at an initial plating density of 100/mm^2. Cultures were used for electrophysiology 8–17 days following plating.

Electrophysiology

Whole-cell recordings were obtained using pipettes with 1.5–4 MΩ open tip resistance when filled with the standard pipette solution containing (in mM): KCl, 130; NaCl, 5.0; $CaCl_2$, 0.5; EGTA, 5.0; and HEPES, 10.0 (pH adjusted to 7.25 with KOH). At the time of experiments, culture medium was replaced with an extracellular recording saline consisting of (in mM): NaCl, 138; KCl, 4.0; $CaCl_2$, 2.0; $MgCl_2$, 1.0; glucose, 10.0; and HEPES, 10.0 (pH 7.25 with NaOH). Except for experiments in which NMDA receptor–mediated EPSCs were specifically examined, 25.0 μM D-APV was included in the bath solution. For examination of responses to exogenous NMDA responses, the bath solution contained 0.5 mM $CaCl_2$, no added $MgCl_2$, 10.0 μM glycine, and 5.0 μM NBQX. Other alterations to these standard solutions are given in the text and figure legends.

Autaptic release of neurotransmitter was stimulated in voltage clamped solitary microculture neurons with a 2.0 ms voltage pulse to 0 mV. Holding potential before and after the stimulus was −70 mV, except as noted. PSCs are totally eliminated with application of saturating concentrations of TTX (1.0 μM; data not shown), suggesting that this stimulation protocol elicits an action potential in the partially clamped axon of the neuron that triggers transmitter release. Stimulation rates for all experiments were <0.05 Hz. Three to six traces in each experimental condition were typically acquired for analysis. Control conditions were interleaved with experimental conditions wherever possible to account for any time-dependent changes in transmission. EPSCs were easily distinguished from

GABAergic IPSCs on the basis of PSC time course. Previous experiments have shown that all PSCs in postnatal hippocampal microcultures are either glutamatergic or GABAergic, defined by sensitivity to appropriate receptor antagonists (Mennerick et al., 1995).

For measurement of steady-state inactivation curves, nucleated patches were excised from solitary microculture neurons (Sather et al., 1992) following synaptic stimulation to identify the transmitter phenotype of the neuron. For these experiments, the pipette solution contained cesium methanesulfonate in place of KCl to block voltage-gated potassium conductances. The extracellular solution also contained 100 μM Cd^{2+} to block Ca^{2+} conductances. The membrane potential was stepped from the holding potential of −70 mV to prepulse potentials ranging from −110 mV to −20 mV for 140 ms, followed by a test activation step to +10 mV. The family of voltage pulses was performed in control, riluzole (20.0 μM), and TTX (500 nM) conditions. The TTX series was digitally subtracted from the control and riluzole series to eliminate any remaining voltage-gated conductances from the analyzed traces.

Data were collected using an Axoclamp 1-D patch-clamp amplifier (Axon Instruments, Foster City, CA) interfaced to a Digidata 1200 acquisition board and a Pentium II computer. Synaptic responses were sampled at 5–10 kHz. Sodium currents from nucleated patches were sampled at 10 kHz. The PClamp software suite (Axon Instruments) was used for data acquisition and analysis. Data were plotted using Sigma Plot (SPSS software). Data are presented in the text and figures as mean ± standard error.

Action potential waveforms in response to depolarizing current injections were measured using the fast current-clamp mode of an EPC9 amplifier. Action potential width was measured at 50% of the peak amplitude. Threshold was defined as the first point at which the slope of the action potential waveform increased by four standard deviations over the average slope during the initial passive membrane response to the depolarizing current injection.

Chemicals and Drugs

All chemicals and solutions were from RBI/Sigma (St. Louis, MO), except for lamotrigine, which was a gift of Dr. Nuri Farber (Washington University). Riluzole, phenytoin, lamotrigine, and carbemazepine were prepared as concentrated stock solutions in dimethyl sulfoxide (DMSO), from which working solutions were prepared. In all cases, DMSO concentration in working solutions was ≤0.1%. TTX and MK-801 were prepared as a stock solution in water and diluted 100- to 5000-fold to achieve working concentrations. Drugs were applied to cells using a multibarrel local perfusion pipette with a common delivery port.

Acknowledgments

The authors thank Joel Springer (University of Kentucky), members of the Zorumski Laboratory, Peter Lukasiewicz, Kel Yamada, Liu Lin Thio (Washington University), and Jack Waters (Stanford University) for valuable discussions and Ann Benz for preparation of hippocampal cultures. The authors are especially indebted to Chuck Zorumski for generous financial and intellectual support. This work was supported by a National Alliance for Research on Schizophrenia and Depression Young Investigator Award (S. M.) and National Institutes of Health grant MH45493.

Received December 21, 1999; revised April 13, 2000.

References

Atwood, H.L. (1967). Variation in physiological properties of crustacean motor synapses. Nature *215*, 57–58.

Bekkers, J.M., and Stevens, C.F. (1991). Excitatory and inhibitory autaptic currents in isolated hippocampal neurons maintained in cell culture. Proc. Natl. Acad. Sci. USA *88*, 7834–7838.

Colbert, C.M., and Johnston, D. (1996). Axonal action-potential initiation and Na^+ channel densities in the soma and axon initial segment of subicular pyramidal neurons. J. Neurosci. *16*, 6676–6686.

Debono, M.W., Le Guern, J., Canton, T., Doble, A., and Pradier, L. (1993). Inhibition by riluzole of electrophysiological responses mediated by rat kainate and NMDA receptors expressed in Xenopus oocytes. Eur. J. Pharmacol. *235*, 283–289.

Fink, M., Lesage, F., Duprat, F., Heurteaux, C., Reyes, R., Fosset, M., and Lazdunski, M. (1998). A neuronal two P domain K^+ channel stimulated by arachidonic acid and polyunsaturated fatty acids. EMBO J. *17*, 3297–3308.

Hashimoto, K., and Kano, M. (1998). Presynaptic origin of paired-pulse depression at climbing fibre-Purkinje cell synapses in the rat cerebellum. J. Physiol. (Lond) *506*, 391–405.

Hebert, T., Drapeau, P., Pradier, L., and Dunn, R.J. (1994). Block of the rat brain IIA sodium channel alpha subunit by the neuroprotective drug riluzole. Mol. Pharmacol. *45*, 1055–1060.

Hessler, N.A., Shirke, A.M., and Malinow, R. (1993). The probability of transmitter release at a mammalian central synapse. Nature *366*, 569–572.

Hille, B. (1992). Ionic Channels of Excitable Membranes (Sunderland, MA: Sinauer Associates).

Hsu, S.F., Augustine, G.J., and Jackson, M.B. (1996). Adaptation of Ca^{2+}-triggered exocytosis in presynaptic terminals. Neuron *17*, 501–512.

Huang, C.S., Song, J.H., Nagata, K., Yeh, J.Z., and Narahashi, T. (1997). Effects of the neuroprotective agent riluzole on the high voltage-activated calcium channels of rat dorsal root ganglion neurons. J. Pharmacol. Exp. Ther. *282*, 1280–1290.

Huettner, J.E., and Bean, B.P. (1988). Block of N-methyl-D-aspartate-activated current by the anticonvulsant MK-801: selective binding to open channels. Proc. Natl. Acad. Sci. USA *85*, 1307–1311.

Johannes, L., Lledo, P.M., Chameau, P., Vincent, J.D., Henry, J.P., and Darchen, F. (1998). Regulation of the Ca^{2+} sensitivity of exocytosis by Rab3a. J. Neurochem. *71*, 1127–1133.

Kilbride, J., Huang, L.Q., Rowan, M.J., and Anwyl, R. (1998). Presynaptic inhibitory action of the group II metabotropic glutamate receptor agonists, LY354740 and DCG-IV. Eur. J. Pharmacol. *356*, 149–157.

Leach, M.J., Marden, C.M., and Miller, A.A. (1986). Pharmacological studies on lamotrigine, a novel potential antiepileptic drug: II. neurochemical studies on the mechanism of action. Epilepsia *27*, 490–497.

Leach, M.J., Baxter, M.G., and Critchley, M.A. (1991). Neurochemical and behavioral aspects of lamotrigine. Epilepsia *32*, S4–S8.

Louvel, E., Hugon, J., and Doble, A. (1997). Therapeutic advances in amyotrophic lateral sclerosis. Trends Pharmacol. Sci. *18*, 196–203.

MacIver, M.B., Amagasu, S.M., Mikulec, A.A., and Monroe, F.A. (1996). Riluzole anesthesia: use-dependent block of presynaptic glutamate fibers. Anesthesiology *85*, 626–634.

Mackenzie, P.J., and Murphy, T.H. (1998). High safety factor for action potential conduction along axons but not dendrites of cultured hippocampal and cortical neurons. J. Neurophysiol. *80*, 2089–2101.

Magee, J.C., and Johnston, D. (1995). Synaptic activation of voltage-gated channels in the dendrites of hippocampal pyramidal neurons. Science *268*, 301–304.

Magleby, K.L. (1987). Short-term changes in synaptic efficacy. In Synaptic Function, G.M. Edelman et al., eds. (New York: John Wiley and Sons), pp. 13–31.

Martin, D., Thompson, M.A., and Nadler, J.V. (1993). The neuroprotective agent riluzole inhibits release of glutamate and aspartate from slices of hippocampal area CA1. Eur. J. Pharmacol. *250*, 473–476.

Martina, M., and Jonas, P. (1997). Functional differences in Na^+ channel gating between fast-spiking interneurones and principal neurones of rat hippocampus. J. Physiol. (Lond) *505*, 593–603.

Martina, M., Vida, I., and Jonas, P. (2000). Distal initiation and active propagation of action potentials in interneuron dendrites. Science *287*, 295–300.

Mennerick, S., and Zorumski, C.F. (1995). Paired-pulse modulation of fast excitatory synaptic currents in microcultures of rat hippocampal neurons. J. Physiol. (Lond) *488*, 85–101.

Mennerick, S., Que, J., Benz, A., and Zorumski, C.F. (1995). Passive and synaptic properties of neurons grown in microcultures and in mass cultures. J. Neurophysiol. *73*, 320–332.

Msghina, M., Govind, C.K., and Atwood, H.L. (1998). Synaptic structure and transmitter release in crustacean phasic and tonic motor neurons. J. Neurosci. *18*, 1374–1382.

Msghina, M., Millar, A.G., Charlton, M.P., Govind, C.K., and Atwood, H.L. (1999). Calcium entry related to active zones and differences in transmitter release at phasic and tonic synapses. J. Neurosci. *19*, 8419–8434.

Murthy, V.N., Sejnowski, T.J., and Stevens, C.F. (1997). Heterogeneous release properties of visualized individual hippocampal synapses. Neuron *18*, 599–612.

Obrenovitch, T.P. (1998). Amyotrophic lateral sclerosis, excitotoxicity and riluzole. Trends Pharmacol. Sci. *19*, 9–11.

Rosenmund, C., Clements, J.D., and Westbrook, G.L. (1993). Nonuniform probability of glutamate release at a hippocampal synapse. Science *262*, 754–757.

Sather, W., Dieudonne, S., MacDonald, J.F., and Ascher, P. (1992). Activation and desensitization of N-methyl-D-aspartate receptors in nucleated outside-out patches from mouse neurones. J. Physiol. (Lond) *450*, 643–672.

Schikorski, T., and Stevens, C.F. (1997). Quantitative ultrastructural analysis of hippocampal excitatory synapses. J. Neurosci. *17*, 5858–5867.

Song, J.H., Huang, C.S., Nagata, K., Yeh, J.Z., and Narahashi, T. (1997). Differential action of riluzole on tetrodotoxin-sensitive and tetrodotoxin-resistant sodium channels. J. Pharmacol. Exp. Ther. *282*, 707–714.

Stefani, A., Spadoni, F., and Bernardi, G. (1997). Differential inhibition by riluzole, lamotrigine, and phenytoin of sodium and calcium currents in cortical neurons: implications for neuroprotective strategies. Exp. Neurol. *147*, 115–122.

Stuart, G.J., and Sakmann, B. (1994). Active propagation of somatic action potentials into neocortical pyramidal cell dendrites. Nature *367*, 69–72.

Stuart, G., Spruston, N., Sakmann, B., and Hausser, M. (1997). Action potential initiation and backpropagation in neurons of the mammalian CNS. Trends Neurosci. *20*, 125–131.

Taylor, C.P., and Meldrum, B.S. (1995). Na^+ channels as targets for neuroprotective drugs. Trends Pharmacol. Sci. *16*, 309–316.

Umemiya, M., and Berger, A.J. (1995). Inhibition by riluzole of glycinergic postsynaptic currents in rat hypoglossal motoneurones. Br. J. Pharmacol. *116*, 3227–3230.

Zucker, R.S. (1989). Short-term synaptic plasticity. Annu. Rev. Neurosci. *12*, 13–31.